Beryllium-boron relative sensitivity factors for melilitic glasses measured with a NanoSIMS ion microprobe

Kohei Fukuda,[1]* Wataru Fujiya,[2] Hajime Hiyagon,[1] Yoshiki Makino,[4] Naoji Sugiura,[1] Naoto Takahata,[3] Takafumi Hirata[4] and Yuji Sano[3]

[1]Department of Earth and Planetary Science, The University of Tokyo, Bunkyo-ku, Tokyo 113-0033, Japan
[2]College of Science, Ibaraki University, Mito, Ibaraki 310-8512, Japan
[3]Atmosphere and Ocean Research Institute, The University of Tokyo, Kashiwa, Chiba 277-8564, Japan
[4]Geochemical Research Center, The University of Tokyo, Bunkyo-ku, Tokyo 113-0033, Japan

The short-lived radionuclide ^{10}Be ($t_{1/2}$ = 1.4 Myr) present in the Early Solar System (ESS) provides important information about the astrophysical environment in which the solar system formed. However, the origin of ^{10}Be in the ESS remains controversial. To reveal its origin, it is important to determine precise and accurate ^{10}Be abundances in meteoritic components. The initial ^{10}Be/^{9}Be ratio can be estimated using ion microprobe analysis and a ^{10}B/^{11}B-^{9}Be/^{11}B correlation. The relative sensitivities for Be and B must be determined to obtain ^{9}Be/^{11}B ratios of unknowns. Here, we report Be/B relative sensitivities for synthetic melilitic glasses and silica-rich NIST SRM 610 glass measured with a NanoSIMS ion microprobe. The Be/B relative sensitivities for melilitic glasses are identical to that of the NIST 610 glass within uncertainties, which suggests that the matrix effects, at least between the NIST 610 glass and melilite, are not significant with respect to Be-B measurements. The present results confirm that the observed variations in the ^{10}Be/^{9}Be ratios for CV calcium-aluminum-rich inclusions (CAIs) are real and the origin of ^{10}Be must be attributed to irradiation by the active early sun. It is also inferred that the ^{10}Be/^{9}Be ratios of fractionation and unidentified nuclear effect (FUN) CV CAIs are not significantly lower than those for normal (non-FUN) CV CAIs, suggesting similar formation conditions.

Keywords: secondary ion mass spectrometry, Berrylium-10, relative sensitivity, melilite, early solar system

INTRODUCTION

Beryllium-10, which decays to ^{10}B with a half-life of 1.4 Myr (Korschinek *et al.*, 2010), cannot be produced by thermonuclear reactions in stars but by spallation reactions induced by galactic and/or stellar cosmic rays (e.g., McKeegan *et al.*, 2000; Desch *et al.*, 2004). Previous Be-B measurements on calcium-aluminum-rich inclusions (CAIs), which are believed to be the earliest solids in the Early Solar System (ESS; Amelin *et al.*, 2010), have demonstrated that this short-lived radionuclide was present in the ESS with initial ^{10}Be/^{9}Be ratios ranging from 1.3×10^{-4} to 1.0×10^{-2} (McKeegan *et al.*, 2000; Sugiura *et al.*, 2001; MacPherson *et al.*, 2003; Chaussidon *et al.*, 2006; Liu *et al.*, 2010; Wielandt *et al.*, 2012; Srinivasan and Chaussidon, 2013; Gounelle *et al.*, 2013; Dunham *et al.*, 2016, 2017; Liu *et al.*, 2017; Sossi *et al.*, 2017). However, the origin of ^{10}Be in the ESS is unknown. Several mechanisms have been suggested for the origin of ^{10}Be including enhanced trapping of galactic cosmic rays (GCRs) in the collapsing cloud core (Desch *et al.*, 2004), solar cosmic ray irradiation (e.g., McKeegan *et al.*, 2000), and stellar processes with neutrino reactions in a relatively low-mass supernova (Banerjee *et al.*, 2016). Varying initial ^{10}Be abundances in CAIs indicate heterogeneous production and/or distribution of ^{10}Be in the ESS, preferring local production of ^{10}Be near the protosun.

Most of the Be-B measurements using secondary ion mass spectrometry (SIMS) have been performed on melilite (solid solution between gehlenite, $Ca_2Al_2SiO_7$, and åkermanite, $Ca_2MgSi_2O_7$) in CAIs into which Be preferentially partitions (Lauretta and Lodders, 1997). With respect to SIMS measurements, the ^{9}Be$^+$/^{11}B$^+$ relative sensitivity factor [RSF: defined by (^{9}Be$^+$/^{11}B$^+$)$_{SIMS}$/(^{9}Be/^{11}B)$_{TRUE}$] of melilite is necessary to calculate the Be/B ratios using ^{10}B/^{11}B vs. ^{9}Be/^{11}B (isochron) diagrams. In previous studies, the RSF for melilite has been assumed to be the same as that of silica-rich glasses such as the NIST SRM 610 glass (e.g., MacPherson *et al.*, 2003). However, the chemical composition of these standards is considerably different from that of melilite and the above-mentioned assumption might therefore be invalid. Thus, previously reported initial ^{10}Be/^{9}Be ratios may include serious systematic errors. For example, a significant dif-

Table 1. Major element compositions, and Be and B concentrations in synthetic melilitic glasses and NIST 610 glass

Sample	Åk#[1]	MgO wt %	2SD		Al₂O₃ wt %	2SD		SiO₂ wt %	2SD		CaO wt %	2SD		Na₂O wt %	Total wt %	No. of analyses
20-1B	25	3.49	±	0.15	26.78	±	1.46	28.22	±	1.29	40.90	±	0.48	—	99.38	20
30-1B	24	3.16	±	0.23	25.85	±	3.50	29.39	±	3.12	41.24	±	1.55	—	99.64	20
60-1A	25	3.48	±	0.15	26.07	±	0.44	28.72	±	0.51	40.84	±	0.47	—	99.11	20
50-1C	43	5.36	±	0.12	18.27	±	0.68	34.07	±	0.59	41.23	±	0.61	—	98.93	20
70-2A	63	6.74	±	0.16	10.03	±	1.03	41.34	±	1.07	41.52	±	0.64	—	99.63	20
BCR-2G[2]		3.59			13.8			54.3			7.22			3.3		
NIST 612[3]		—			2.06			71.7			11.93			14.0		
NIST 610[4]		0.0057			1.98			69.4			11.59			13.6		

Sample	Be (ppm)	2SD[5]		B (ppm)	2SD[5]		No. of analyses
20-1B	912	±	34	79	±	3	7
30-1B	901	±	69	58	±	6	10
60-1A	2204	±	205	69	±	10	3
50-1C	1547	±	107	58	±	10	4
70-2A	2188	±	122	58	±	6	5
BCR-2G[2]	2.1	±	0.5	7.2	±	1	1
NIST 612[3]	39	±	3	35	±	3	5
NIST 610[4]	476			350			

*[1] Åk#: approximate åkermanite numbers, calculated from Mg(cation)/(Mg(cation)+Al(cation)/2).
*[2] Major element concentrations from Jochum et al. (2005). *[3] Major element concentrations from Jochum et al. (2011).
*[4] Major elements, Be, and B concentrations from Jochum et al. (2011).
*[5] Errors of BCR-2G are counting errors (2σ) because the sample was measured only 1 spot.

Table 2. Ion intensity ratios measured with the NanoSIMS and the calculated relative sensitivity factors

Sample	Åk#	$^9Be/^{11}B$ atomic ratios (atomic ratio)[*2]			No. of analyses	$^9Be^+/^{11}B^+$ (ion intensity ratio)[*3]			No. of analyses	RSF[*1]		
20-1B	25	17.3	±	0.6	7	44.3	±	2.2	4	2.57	±	0.16
30-1B	24	23.3	±	1.6	10	57.6	±	2.9	4	2.47	±	0.21
60-1A	25	48.2	±	6.9	3	135.9	±	6.9	3	2.82	±	0.43
50-1C	43	40.4	±	4.8	4	100.0	±	11.3	4	2.48	±	0.40
70-2A	63	56.4	±	4.6	5	145.9	±	11.5	4	2.59	±	0.30
weighted mean										**2.55**	**±**	**0.11**
NIST 610		2.03				4.98	±	0.25	11	2.44	±	0.12

[*1]*Relative sensitivity factor: $(^9Be^+/^{11}B^+)_{NanoSIMS}/(^9Be/^{11}B)_{atomic}$. Errors are 2σ.*
[*2]*Calculated from Be and B concentrations in Table 1 assuming terrestrial isotopic ratios. Errors are 2σ.*
[*3]*Errors are 2 Standard Deviation (2SD). If 2SD errors are smaller than the reproducibility of NIST 610 (2SD), the latter was adopted.*

ference in the Mn/Cr RSF was observed between silicates and carbonates, which resulted in significant errors in the Mn-Cr ages for carbonates (Sugiura *et al.*, 2010; Fujiya *et al.*, 2012; Steele *et al.*, 2017). Preliminary results for Be/B RSFs for three melilitic glasses were presented by Fukuda *et al.* (2016). Note that the reported Be/B RSFs in Fukuda *et al.* (2016) are not absolute values because we did not check relative sensitivities between each electron multiplier (EM) during the analysis. In the present study, we conducted more refined measurements on five newly synthesized melilitic glasses using a NanoSIMS (for Be^+/B^+ intensity ratios) and a laser ablation-inductively coupled plasma-mass spectrometer (LA-ICP-MS; for Be/B elemental ratios). We report the revised RSFs, which are essential for the determination of accurate initial abundances of ^{10}Be and to discuss its origin in the ESS.

EXPERIMENTAL

We synthesized five glasses with approximate melilitic compositions and åkermanite numbers (Åk#s; see Table 1 for the definition) ranging from 24 to 63 that were doped with trace amounts of Be and B with varying Be/B ratios (Table 1). The glasses were prepared by melting mixtures of oxide powders. The starting materials were wrapped in Pt-foil, heated, melted with a blowtorch, and quenched by dropping them into Milli-Q water. The synthesized glasses ($\sim500 \times 500$ μm^2) were embedded in epoxy together with a NIST SRM 610 glass standard and then polished. The sample mount was cleaned with Mill-Q water and ethanol to remove surface contamination. The sample was coated with carbon after drying to prevent surface charge during subsequent electron microprobe and SIMS analyses.

The major element concentrations of the synthetic glasses were determined with a JXA-8530F field-emission gun electron microprobe installed at the University

of Tokyo using a 15 kV accelerating voltage, 12 nA beam current, ~1 μm focused beam, and wavelength-dispersive X-ray spectroscopy (WDS). Matrix effects were corrected using the ZAF method. The concentrations of major elements in the synthesized glasses are listed in Table 1. The approximate Åk#s and Be and B concentrations measured with LA-ICP-MS are also shown.

The ion intensities of Be and B were determined with a NanoSIMS 50 ion probe at the Atmosphere and Ocean Research Institute (AORI) of the University of Tokyo. The NanoSIMS measurements were performed in multicollection mode. A $^{16}O^-$ primary ion beam (~1 nA intensity and ~5 μm in diameter) was rastered over 10×10 μm^2 areas (32×32 pixels with a dwell time of 200 μs/pixel) to stabilize the secondary ion intensities. To remove the carbon coating and surface contamination before each analysis, a ~1 nA primary ion beam was rastered over 10×10 μm^2 areas for ~10 min. Secondary ions of $^9Be^+$, $^{10}B^+$, $^{11}B^+$, and $^{30}Si^+$ were then detected simultaneously with secondary electron multipliers (EMs). The measurements were performed with a mass resolving power (MPR) of 1500 at a peak height of 1%. The intensities of $^9Be^+$, $^{11}B^+$, and $^{30}Si^+$ were $(2.1–3.8) \times 10^4$ cps, $(0.3–6.0) \times 10^3$ cps, and $(0.1–1.7) \times 10^5$ cps, respectively. An electronic beam blanking mode was applied such that only signals from the central 24×24 pixel area were collected. This blanking helped to avoid contributions from scattered ions from the surroundings. The relative sensitivities between the EMs used for the Be and B measurements were checked after the measurement and corrected to calculate RSFs. The dead time (~44 ns) of the counting system was also corrected. The EM background (much lower than ~0.05 cps) was not corrected because it was negligible compared with the count rates of ^9Be and ^{11}B for the samples. Measurements on synthetic melilitic glasses were conducted only near the center of the individual glasses.

After the NanoSIMS analyses, the Be and B concen-

trations near NanoSIMS analysis spots on the same glasses were determined using a LA-ICP-MS. Laser ablation was performed with an in-house laser ablation system (Cyber Probe) combined with a titanium-sapphire (Ti:S) femtosecond laser (IFRIT, Cyber Laser, Japan) and galvano metric fast scanning laser system (Yokoyama *et al.*, 2011; Makino *et al.*, 2017). A single quadrupole mass spectrometer (iCAP Qc, Thermo Fisher Scientific, USA) was utilized. The LA-ICP-MS measurements were performed in spot analysis mode. We obtained ion intensities for $^{7}Li^{+}$, $^{9}Be^{+}$, $^{10}B^{+}$, $^{11}B^{+}$, $^{24}Mg^{+}$, $^{29}Si^{+}$, and $^{43}Ca^{+}$. Ablation pits of ~25 μm in diameter were produced by fast circular scanning of a laser beam with a diameter of 10 μm. The scanning repetition rate and laser fluence were optimized to obtain maximum signal intensities for ^{238}U and ^{11}B using NIST SRM 610 as a standard. The NIST 610 glass was also used as reference for the correction of the relative sensitivities of Be, B, and Ca. The Be and B concentrations were determined using the observed $^{9}Be^{+}/^{43}Ca^{+}$ and $^{11}B^{+}/^{43}Ca^{+}$ intensity ratios and ^{43}Ca concentrations (calculated from total Ca concentrations assuming normal isotopic ratios) of the samples. The NIST SRM 612 and BCR-2G glasses were measured as secondary standards. The instrumentation and detailed analytical conditions are summarized in Supplementary Table S1.

RESULTS

The Be and B concentrations in the melilitic glasses obtained from LA-ICP-MS analyses are listed in Table 1. To verify the accuracy of the Be and B concentrations in the melilitic glasses, we also measured NIST 612 and BCR-2G glasses as secondary standards under the same analytical conditions. The Be and B concentrations of the NIST 612 and BCR-2G glasses are consistent with literature values (Jochum *et al.*, 2011; Jacob, 2006), which justifies the current LA-ICP-MS analysis (see Table 1).

The $^{9}Be/^{11}B$ atomic ratios (calculated from the Be and B concentrations in Table 1), $^{9}Be^{+}/^{11}B^{+}$ ion intensity ratios measured with the NanoSIMS, and corresponding Be/B RSFs calculated for individual glasses are listed in Table 2. Figure 1 shows the $^{9}Be^{+}/^{11}B^{+}$ intensity ratios as a function of atomic $^{9}Be/^{11}B$ ratios. The $^{9}Be^{+}/^{11}B^{+}$ intensity ratios and atomic $^{9}Be/^{11}B$ ratios of the synthesized glasses correlate well. The RSFs calculated for individual glasses are identical within uncertainties (2.47 ± 0.21 to 2.82 ± 0.43). Note that five glasses have different chemical compositions, with Åk# ranging from 24 to 63. The obtained RSFs are independent of the åkermanite numbers. Therefore, we used the weighted mean of the five datapoints and obtained the RSF of 2.55 ± 0.11 (2σ). We also determined the Be/B RSF for NIST SRM 610 under the same analytical conditions. The RSF shows a small day-to-day variation from 2.44 ± 0.12 (2 standard devia-
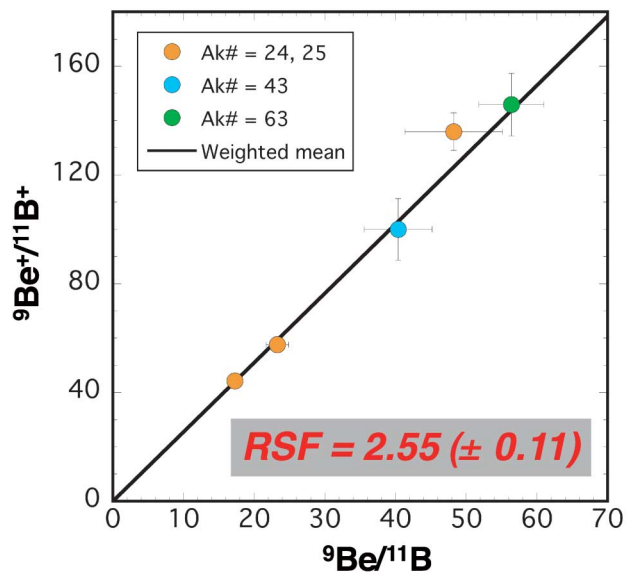

Fig. 1. $^{9}Be^{+}/^{11}B^{+}$ ratios as a function of Be/B atomic ratios determined on five synthetic melilitic glasses. The sensitivity difference between the electron multipliers (EMs) for $^{9}Be^{+}$ and $^{11}B^{+}$ was corrected. The error bars represent 2 standard deviations (SD) evaluated from repeated measurements of individual glasses. The slope defines the weighted mean value of the relative sensitivity of five glasses.

tions, SD) to 2.68 ± 0.05 (2 SD), but the RSF of our melilitic glasses obtained during the analytical period is 2.44 ± 0.12 (2 SD). The present results demonstrate that the Be/B RSF of the synthetic melilitic glasses is identical to that of NIST SRM 610, within uncertainties.

We also determined the RSFs of $^{9}Be/^{30}Si$ and $^{11}B/^{30}Si$ for melilitic glasses and NIST 610. The Be/Si and B/Si RSFs obtained for melilitic glasses are slightly higher than or almost comparable to those of the NIST 610 glass. These observations suggest matrix effects between melilitic glasses and NIST 610 glass, at least for some elements. Therefore, it may be fortuitous that the Be/B RSF does not show noticeable matrix effects between melilitic glasses and NIST 610 glass. Detailed information is reported in Supplementary Materials (Table S2 and Fig. S1).

DISCUSSION

The present results demonstrate that matrix effects do not significantly affect the relative ionization efficiencies of Be and B of the melilitic glasses and NIST 610 glass standard. Hence, the NIST 610 (and 612) glass can be used as a proper standard for accurate Be-B SIMS measurements on melilite in CAIs. Below, we will compare
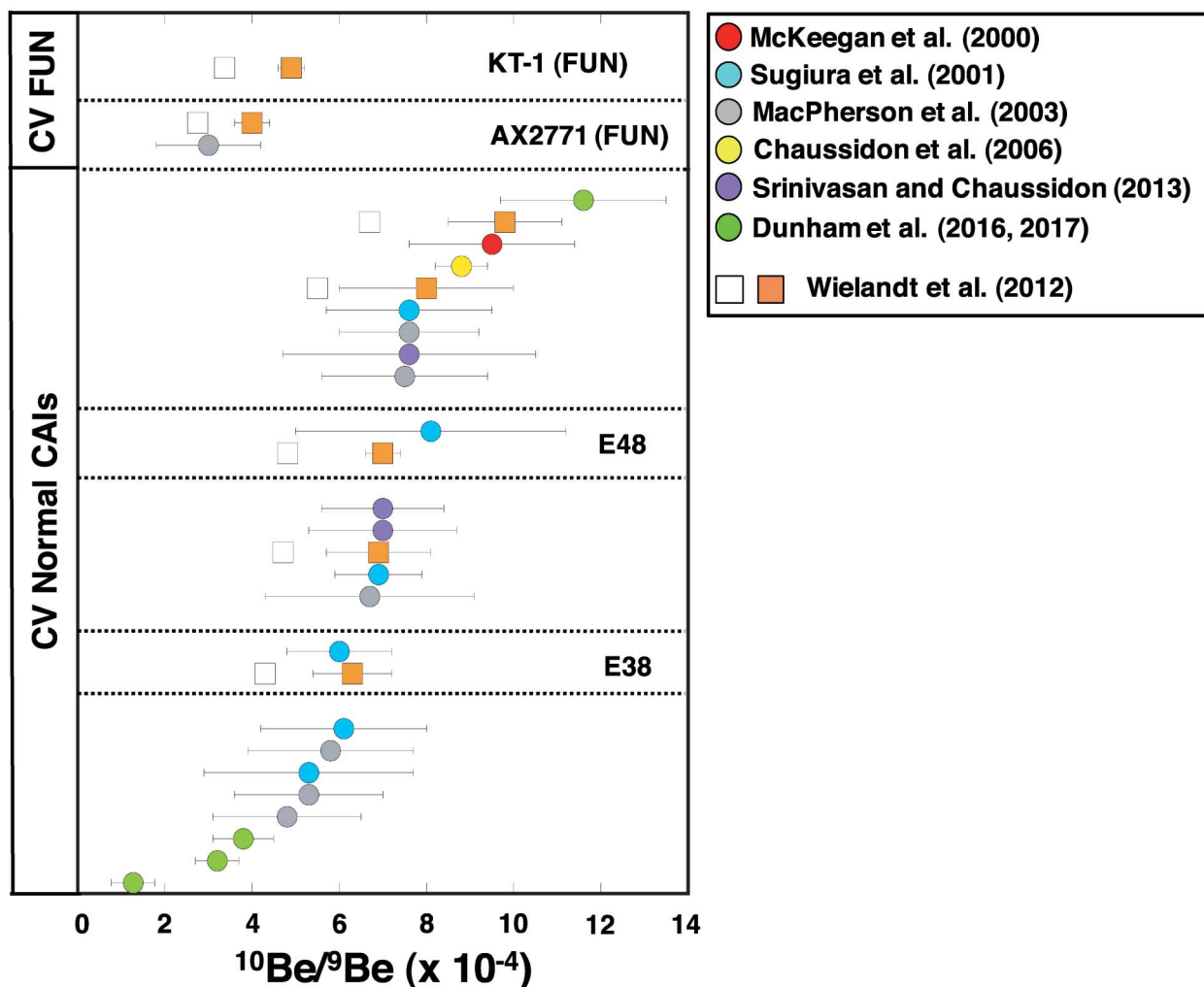
Fig. 2. Compilation of the reported initial $^{10}Be/^{9}Be$ ratios of CV normal and fractionation and unidentified nuclear effect (FUN) CAIs (filled circles: McKeegan et al., 2000; Sugiura et al., 2001; MacPherson et al., 2003; Chaussidon et al., 2006; Srinivasan and Chaussidon, 2013; Dunham et al., 2016, 2017; open squares: Wielandt et al., 2012). The revised initial $^{10}Be/^{9}Be$ ratios (filled squares) are also plotted based on the RSF of the NIST 612 reported by Wielandt et al. (2012; see text). The error bars represent 2σ.

Be-B data previously reported for CV CAIs that were obtained using different standards. If necessary, we will apply appropriate corrections based on the present results.

MacPherson et al. (2003) and Dunham et al. (2016, 2017) used the NIST (NBS) 610 and 612 standards to determine the Be/B RSF and reported initial $^{10}Be/^{9}Be$ ratios of CV CAIs including a few fractionation and unidentified nuclear effect (FUN) CAIs. The initial $^{10}Be/^{9}Be$ ratios vary from 1.3×10^{-4} to 11.6×10^{-4} for normal (i.e., non-FUN) CAIs and $3.0 \pm 1.2 \times 10^{-4}$ (MacPherson et al., 2003) or $<5.8 \times 10^{-4}$ (Dunham et al., 2017) for FUN CAIs. No corrections are needed for these data.

Sugiura et al. (2001) and Wielandt et al. (2012) conducted Be-B measurements on the same CAIs (E38 and E48) from Efremovka. However, the $^{10}Be/^{9}Be$ ratios re-

ported by Sugiura et al. (2001; $6.1 \pm 1.2 \times 10^{-4}$ and $8.1 \pm 3.1 \times 10^{-4}$, respectively) are higher than those reported by Wielandt et al. (2012; $4.43 \pm 0.61 \times 10^{-4}$ and $4.82 \pm 0.25 \times 10^{-4}$, respectively). Wielandt et al. (2012) determined a Be/B RSF of ~2.6 using the NIST SRM glass 612 ($SiO_2 = 71.8$ wt%; Jochum et al., 2011) and ~1.78 using GSC-1G and GSD-1G glasses ($SiO_2 = 52.5$ wt% and 53.0 wt%, respectively; Jochum et al., 2005). The former is in good agreement with our RSFs for NIST glass 610 and melilitic glasses, but the latter is 30% lower than the RSF for our melilitic glasses. Wielandt et al. (2012) adopted the latter RSF, but the present results suggest that the former RSF may be appropriate for accurate Be-B measurements on melilites in CAIs. If we use 2.6 instead of 1.78 as the Be/B RSF, the revised values ($6.3 \pm 0.9 \times$

10^{-4} and $7.0 \pm 0.4 \times 10^{-4}$, respectively) are consistent with those obtained by Sugiura *et al.* (2001), within uncertainties.

Note that the Be/B RSFs for NIST 610 and 612 determined by three different instruments are similar to each other, i.e., ~2.6 (IMS-1280; Wielandt *et al.*, 2012), ~2.5 (IMS-6f; MacPherson *et al.*, 2003), and ~2.44 (NanoSIMS; this study). This suggests that the relative sensitivities of Be and B do not depend much on the ion optics of the instruments but are more intrinsic to sputtering and ionization processes. In fact, Ito and Messenger (2016) also reported similar RSFs for rare earth elements determined by different instruments (IMS-3f, IMS-4f, and NanoSIMS).

Sugiura *et al.* (2001) determined a Be/B RSF of 2.67 ± 0.09 for a suite of geological standards with varying SiO_2 contents (51.0–72.3 wt%; Imai *et al.*, 1995). Although Sugiura *et al.* (2001) did not measure the RSF of NIST glasses, a similar RSF was obtained for the NIST 610 and 612 glasses using the same instrument (IMS-6f; MacPherson *et al.*, 2003). Hence, the $^{10}Be/^{9}Be$ ratios reported in Sugiura *et al.* (2001) may not need corrections. Note that our melilitic glasses and NIST 610 measured in this study also have varying SiO_2 contents (28.2–41.3 wt% and 69.4 wt%, respectively). This suggests that the Be/B RSF is rather insensitive to the SiO_2 content.

McKeegan *et al.* (2000) and Chaussidon *et al.* (2006) used a synthetic GB4 glass standard (SiO_2 = 72.9 wt%; Gurenko *et al.*, 2005) and measured Be-B isotopes in CV CAIs with an IMS-1270 ion microprobe. The Be/B RSF measured by Chaussidon *et al.* (2006) varies from 2.51 to 2.88 (with an average of 2.73), which overlaps with that of NIST glass standards determined by three different instruments, as described above. Therefore, these data may not need corrections. Recently, Sossi *et al.* (2017) also used the GB4 standard for the Be-B analysis of CV CAIs. However, their Be/B RSF (~3.17) is significantly higher than that of GB4 determined by Chaussidon *et al.* (2006) or that of silica-rich NIST glasses obtained by other researchers (see above). The cause for this difference is uncertain but may be attributed to different analytical conditions. In this case, we cannot make proper corrections.

Figure 2 summarizes initial $^{10}Be/^{9}Be$ ratios previously reported for CV normal and FUN CAIs (filled symbols). The original data of Wielandt *et al.* (2012) are shown as open symbols and the corrected data, assuming a Be/B RSF of 2.6, are displayed as filled symbols. Note that the data for FUN CAIs were relatively low (2.8×10^{-4} to 3.4×10^{-4}; Wielandt *et al.*, 2012) before correction. However, they are much higher after correction (4.0×10^{-4} to 4.9×10^{-4}). Based on the original data, Wielandt *et al.* (2012) and Tatischeff *et al.* (2014) suggested that the $^{10}Be/^{9}Be$ ratios recorded on FUN CAIs represent the baseline level present in the protosolar molecular cloud. However, the corrected $^{10}Be/^{9}Be$ ratios of FUN CAIs are higher than that of the baseline level of the molecular cloud (~1.3×10^{-4} to 3.4×10^{-4}; Tatischeff *et al.*, 2014) and within the range of normal CV CAIs (see Fig. 2). Furthermore, Dunham *et al.* (2017) recently reported a very low $^{10}Be/^{9}Be$ ratio of $1.27 \pm 0.50 \times 10^{-4}$ for a normal CV CAI (B4), that is, much lower than the corrected $^{10}Be/^{9}Be$ ratios of CV FUN CAIs. These observations indicate that the initial $^{10}Be/^{9}Be$ ratios of CV FUN CAIs cannot be explained by a baseline level of ^{10}Be abundances in the protosolar molecular cloud.

Previous studies indicated a large variation in the $^{10}Be/^{9}Be$ ratios of CV CAIs, from 1.3 to 11.6×10^{-4} (McKeegan *et al.*, 2000; Sugiura *et al.*, 2001; MacPherson *et al.*, 2003; Chaussidon *et al.*, 2006; Wielandt *et al.*, 2012; Srinivasan and Chaussidon, 2013; Dunham *et al.*, 2016, 2017). The present results confirm that most of the previous data may not need corrections. Hence, the variation in the $^{10}Be/^{9}Be$ ratios of CV CAIs is real. Note that the data for other types of refractory inclusions, such as hibonite and grossite inclusions, also show a large variation in the $^{10}Be/^{9}Be$ ratios, from 5.3×10^{-4} to 100×10^{-4} (Liu *et al.*, 2010; Gounelle *et al.*, 2013). These data, however, must be re-evaluated because the Be/B RSFs for hibonite and grossite may, in principle, not be identical to those of melilite or NIST standard glasses, especially considering that hibonite and grossite are non-silicate minerals. The observed variation in the $^{10}Be/^{9}Be$ ratios suggests the local production of ^{10}Be, which is consistent with the production of ^{10}Be by solar cosmic ray irradiation (e.g., McKeegan *et al.*, 2000).

CONCLUSIONS

In this study, we synthetized five melilitic glasses and investigated the Be/B RSFs of these glasses using a NanoSIMS 50 and LA-ICP-MS. We found that the Be/B RSFs of melilitic glasses (1) are independent of the Åk#; (2) identical to that for NIST 610 silica-rich glass, within uncertainties; and (3) after proper correction of previous data based on the present results, the revised $^{10}Be/^{9}Be$ ratios of CV FUN CAIs are higher and well within the range of $^{10}Be/^{9}Be$ ratios of CV normal CAIs. Hence, the $^{10}Be/^{9}Be$ ratios of CV FUN CAIs may not represent a baseline level of ^{10}Be abundances in the protosolar molecular cloud, suggesting similar formation processes of both FUN and normal (non-FUN) CAIs, possibly due to solar cosmic ray irradiation.

REFERENCES

Amelin, Y., Kaltenbach, A., Iizuka, T., Stirling, C. H., Ireland, T. R., Petaev, M. and Jacobsen, S. B. (2010) U-Pb chronology of the solar system's oldest solids with variable $^{238}U/^{235}U$. *Earth Planet. Sci. Lett.* **300**, 343–350.

Banerjee, P., Qian, Y.-Z., Heger, A. and Haxton, W. C. (2016) Evidence from stable isotopes and ^{10}Be for solar system formation triggered by a low-mass supernova. *Nat. Commun.* **7**, 13639.

Chaussidon, M., Robert, F. and McKeegan, K. D. (2006) Li and B isotopic variations in an Allende CAI: Evidence for the in situ decay of short-lived ^{10}Be and for the possible presence of the short-lived nuclide ^{7}Be in the early solar system. *Geochim. Cosmochim. Acta* **70**, 224–245.

Desch, S. J., Connolly, H. C., Jr. and Srinivasan, G. (2004) An interstellar origin for the beryllium 10 in calcium-rich, aluminum-rich inclusions. *Astrophys. J.* **602**, 528–542.

Dunham, E., Wadhwa, M., Simon, S. and Grossman, L. (2016) Beryllium-boron systematics of refractory inclusions in CR2 and CV3 chondrites: evidence for ^{10}Be heterogeneity (abstract). *Meteorit. Planet. Sci.* **79**, #6222.

Dunham, E., Wadhwa, M. and Desch, S. J. (2017) Beryllium-boron systematics of two distinctive CAIs from CV3 chondrites: the relatively pristine CAI B4 from NWA 6991 and the FUN CAI CMS-1 from Allende (abstract). *LPSC* **45**, #2523.

Fujiya, W., Sugiura, N., Hotta, H., Ichimura, K. and Sano, Y. (2012) Evidence for the late formation of hydrous asteroids from young meteoritic carbonates. *Nat. Commun.* **3**, 627.

Fukuda, K., Fujiya, W., Hiyagon, H., Sugiura, N., Takahata, N. and Sano, Y. (2016) An ion microprobe study of Be-B isotope systematics in melilite-rich CAIs based on newly determined Be/B relative sensitivity factors for melilitic glass (abstract). *Meteorit. Planet. Sci.* **79**, #6459.

Gounelle, M., Chaussidon, M. and Rollion-Bard, C. (2013) Variable and extreme irradiation conditions in the early solar system inferred from the initial abundance of ^{10}Be in Isheyevo CAIs. *Astrophys. J.* **763**, L33.

Gurenko, A. A., Veksler, I. V., Meixner, A., Thomas, R., Dorfman, A. M. and Dingwell, D. B. (2005) Matrix effect and partitioning of boron isotopes between immiscible Si-rich and B-rich liquids in the Si-Al-B-Ca-Na-O system: A SIMS study of glasses quenched from centrifuge experiments. *Chem. Geol.* **222**, 268–280.

Imai, N., Terashima, S., Itoh, S. and Ando, A. (1995) Compilation of analytical data for minor and trace elements in seventeen GSJ geochemical reference samples, "igneous rock series". *Geostandard Newslett.* **19**, 135–213.

Ito, M. and Messenger, S. (2016) Rare earth element measurements and mapping of minerals in the Allende CAI, 7R19-1, by NanoSIMS ion microprobe. *Meteorit. Planet. Sci.* **51**, 818–832.

Jacob, D. E. (2006) High sensitivity analysis of trace element-poor geological reference glasses by Laser Ablation-Inductively Coupled Plasma-Mass Spectrometry (LA-ICP-MS). *Geostand. Geoanal. Res.* **30**, 221–235.

Jochum, K. P., Willbold, M., Raczek, I., Stoll, B. and Herwig, K. (2005) Chemical Characteristation of the USGS Reference Glasses GSA-1G, GSC-1G, GSD-1G, GSE-1G, BCR-2G, BHVO-2G and BIR-1G Using EPMA, ID-TIMS, ID-ICP-MS and LA-ICP-MS. *Geostand. Geoanal. Res.* **29**, 285–302.

Jochum, K. P., Weis, U., Stoll, B., Kuzmin, D., Yang, Q., Raczek, I., Jacob, D. E., Stracke, A., Birbaum, K., Frick, D. A., Günther, D. and Enzweiler, J. (2011) Determination of reference values for NIST SRM 610-617 glasses following ISO guidelines. *Geostand. Geoanal. Res.* **35**, 397–429.

Korschinek, G., Bergmaier, A., Faestermann, T., Gerstmann, U. C., Knie, K., Rugel, G., Wallner, A., Dillmann, I., Dollinger, G., Lierse von Gostomski, C., Kossert, K., Maiti, M., Poutivtsev, M. and Remmert, A. (2010) A new value for the half-life of ^{10}Be by Heavy-Ion Elastic Recoil Detection and liquid scintillation counting. *Nucl. Instrum. Methods Phys. Res. B* **268**, 187–191.

Lauretta, D. S. and Lodders, K. (1997) The cosmochemical behavior of beryllium and boron. *Earth Planet. Sci. Lett.* **146**, 315–327.

Liu, M.-C., Nittler, L. R., Alexander, C. M. O. and Lee, T. (2010) Lithium-beryllium-boron isotopic compositions in meteoritic hibonite: implications for origin of ^{10}Be and early solar system irradiation. *Astrophys. J.* **719**, L99–L103.

Liu, M.-C., Han, J. and Brearley, A. (2017) The boron isotopic ratios of a fine-grained inclusion from the Allan Hills 77307 chondrite (CO3.0) (abstract). *Meteorit. Planet. Sci.* **80**, #6291.

MacPherson, G. J., Huss, G. R. and Davis, A. M. (2003) Extinct ^{10}Be in type A Calcium-Aluminum-rich inclusions from CV chondrites. *Geochim. Cosmochim. Acta* **67**, 3165–3179.

Makino, Y., Ohara, S., Yamada, M., Mukoyama, S., Hattori, K., Sakata, S., Tanaka, Y., Suzuki, T., Shinohara, A., Matsukawa, T., Yokoyama, K. and Hirata, T. (2017) Quantitative elemental bioimaging protocol using femtosecond-laser ablation-ICP-mass spectrometry coupled with glass standard reference material. *Metallomics—Recent Analytical Techniques and Applications*, Springer, 93–106.

McKeegan, K. D., Chaussidon, M. and Robert, F. (2000) Incorporation of short-lived ^{10}Be in a Calcium-Aluminum-rich inclusion from the Allende meteorite. *Science* **289**, 1334–1337.

Sossi, P. A., Moynier, F., Chaussidon, M., Villeneuve, J., Kato, C. and Gounelle, M. (2017) Early solar system irradiation quantified by linked vanadium and beryllium isotope variations in meteorites. *Nat. Astron.* **1**, 0055.

Srinivasan, G. and Chaussidon, M. (2013) Constraints on ^{10}Be and ^{41}Ca distribution in the early solar system from ^{26}Al and ^{10}Be studies of Efremovka CAIs. *Earth Planet. Sci. Lett.* **374**, 11–23.

Steele, R. C. J., Heber, V. S. and McKeegan, K. D. (2017) Matrix effects on the relative sensitivity factors for manganese and chromium during ion microprobe analysis of carbon-

ate: Implications for early Solar System chronology. *Geochim. Cosmochim. Acta* **201**, 245–259.

Sugiura, N., Shuzou, Y. and Ulyanov, A. (2001) Beryllium-boron and aluminum-magnesium chronology of calcium-aluminum-rich inclusions in CV chondrites. *Meteorit. Planet. Sci.* **36**, 1397–1408.

Sugiura, N., Ichimura, K., Fujiya, W. and Takahata, N. (2010) Mn/Cr relative sensitivity factors for synthetic calcium carbonate measured with a NanoSIMS ion microprobe. *Geochem. J.* **44**, e11–e16.

Tatischeff, V., Duprat, J. and de Séréville, N. (2014) Light-element nucleosynthesis in a molecular cloud interacting with a supernova remnant and the origin of beryllium-10 in the protosolar nebula. *Astrophys. J.* **796**, 124 (20 pp.).

Wielandt, D., Nagashima, K., Krot, A. N. and Huss, G. R. (2012) Evidence for multiple sources of ^{10}Be in the early solar system. *Astrophys. J.* **748**, L25.

Yokoyama, T. D., Suzuki, T., Kon, Y. and Hirata, T. (2011) Determinations of rare earth element abundance and U-Pb age of zircon using multispot laser ablation-inductively coupled plasma mass spectrometry. *Anal. Chem.* **83**, 8892–8899.

Supplementary Materials

URL (http://www.terrapub.co.jp/journals/GJ/archives/
data/52/MS510.pdf)
Figure S1
Tables S1 and S2